Inverse photoemission spectroscopy of Al(100)

J. F. Veyan,[1,2] W. Ibañez,[1] R. A. Bartynski,[3] P. Vargas,[1] and P. Häberle[1,*]
[1]*Departamento de Física, Universidad Técnica Federico Santa María, Casilla 110-V, Valparaíso, Chile*
[2]*Instituto de Física, Universidad Católica de Valparaíso, Casilla 4059, Valparaíso, Chile*
[3]*Department of Physics and Astronomy, Rutgers University, Piscataway, New Jersey 08855-0849, USA*
(Received 26 November 2003; revised manuscript received 3 January 2005; published 25 April 2005)

We present results from *k*-resolved inverse photoemission spectroscopy (IPS) in the isochromat mode from the Al(100) surface. To identify the origin of the different peaks in the photon intensity we have performed a first principles calculation of the bulk band structure in the LMTO formalism and apply it to predict bulk derived features in the IPS spectra. We have been able to identify several of the experimental features as derived from bulk optical transitions together with various surface resonances. A particular surface state detected along the $\overline{\Gamma X}$ direction displays the opening of a gap at the zone boundary. Most of the dominant surface features could be traced back to the occupied surface state at $\overline{\Gamma}$, previously detected by photoemission.

DOI: 10.1103/PhysRevB.71.155416 PACS number(s): 73.20.At

I. INTRODUCTION

Al is a very promising material from which nanometer length scale structures could be built. From a fundamental point of view, Al has a simple electronic structure that is well described by the nearly free electron model and thus is an excellent laboratory for understanding new phenomena that emerge in nanoscale confinement.[1,2] To facilitate further applications of this free electron metal in nanoscale systems, it is important to acquire a precise knowledge of its electronic structure, especially the electronic states in the vicinity of the Fermi level (ε_F) which are responsible for transport and excitation phenomena. Recent experiments on thin layers of simple metals,[3–5] probing the coupling between collective electronic excitations and photons, open the possibility that these interesting modes play an important role in the photon field associated with optical transitions in inverse photoemission spectroscopy (IPS). Al is especially interesting since the maximum IPS emission intensity should occur at the multipole plasmon frequency (13 eV) (Ref. 6) and close enough to the 9.5 eV photon energy detected in isochromat IPS.

There have been several reports of experimental measurements of the occupied electronic states of Al,[7–12] including some studies describing the electronic structure above the Fermi level (ε_F).[6,13–18] However, none of these studies have dealt systematically with the unoccupied states of the (100) surface. The work we present here is intended to fill this gap. In this paper we present isochromat IPS measurements, of the unoccupied electronic states of the Al(100) surface along the $\overline{\Gamma X}$ and $\overline{\Gamma M}$ directions of the surface Brillouin zone (SBZ). We find that the spectra often exhibit a number of weak features which can be associated with the bulk electronic structure. Occasionally strong spectral features are observed in regions of energy and momentum space that correspond to projected gaps in the Al band structure. These features are identified as surface states and only appear in rather limited ranges of energy and $k_{\|}$.

For a better description of our experimental measurements, we have also performed numerical calculations of the bulk electronic structure, appropriately modified to directly predict Al bulk optical transitions giving rise to events detectable by isochromat IPS. In this way it is easier to identify both the origin of the spectral feature and its relation to the bulk electronic structure.

II. EXPERIMENT

The sample used in these measurements was a commercially produced Al(100) crystal disk with two unpolished planes aligned parallel to the [100] direction with a precision better than 0.5°. One of the crystal faces was mechanically polished with Al_2O_3 particles down to 0.1 μm. The crystal was then inserted into the ultrahigh vacuum (UHV) experimental chamber, with a base pressure of 1×10^{-10} Torr. Here it was subjected to cycles of Ar sputtering (1 keV) and annealing up to 400 °C, for a total time of approximately 20 h. The crystalline order and cleanliness of the surface were monitored both by using low energy electron diffraction and the normal incidence IPS spectrum. The primary experimental technique housed in the UHV chamber is an isochromat inverse photoemission spectrometer,[19] which has been described in detail elsewhere.[20] The setup is based in a design by Dose.[21] In brief, the spectrometer consists of a bandpass Geiger Müller as a photon detector,[22] which is highly sensitive to photons in a very narrow band around (9.5 ± 0.3) eV. The electron beam is produced by an electron gun, with a BaO cathode, based on a design by Zipf.[23] By adjusting the angle (θ) between the incident electron momentum and the surface normal, it is possible to explore the dispersion of the different states as a function of the momentum parallel to the surface ($\hbar k_{\|}$). To probe the electronic structure along a particular direction of the SBZ, it is then necessary to collect a series of spectra of the photon intensity vs incoming electron energy, for different angles between the electron momentum and the surface normal. The IPS signal has an onset at the Fermi level of the material and this value is usually taken as the origin for measuring the energy of the different spectral features. The electronic parallel momentum and the energy of a resonance are related by

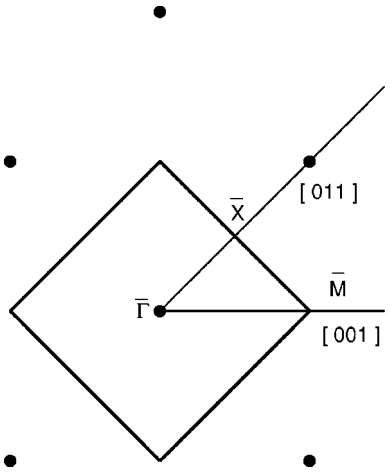

FIG. 1. Representation of the SBZ of the Al(100) surface. The main crystallographic directions are along $\overline{\Gamma X}$ and $\overline{\Gamma M}$.

$$k_{\parallel} = \sin\theta \sqrt{\frac{2m}{\hbar^2}(\varepsilon + \hbar\omega - \phi)},$$

with m being the electron mass, ε the energy of the resonance measured with respect to ε_F, $\hbar\omega$ is the energy of the detected photons, ϕ the work function of the sample [4.4 eV for Al (Ref. 24)], and θ has been defined above.

Figure 1 shows a schematic diagram of the Al(100) surface in reciprocal space. In the vacuum chamber, the crystal was azimuthally aligned in such a way that the high symmetry ($\overline{\Gamma X}$ or $\overline{\Gamma M}$) directions of the SBZ were explored with increasing θ.

III. NUMERICAL CALCULATION

Even though IPS is one of the most direct techniques to explore low energy single electron excitations in crystalline samples, there are some difficulties in interpreting the origin of the different spectral features. For example, distinguishing between a feature associated with a bulk direct transition and one caused by a legitimate surface state (i.e., with a wave function limited to the surface region of the crystal) is no simple task. In part to help us resolve this dilemma, we have performed standard LMTO calculations[25] of the Al bulk electronic structure, with lattice constant $a=4.05$ Å. Details of the application of this method to IPS have been presented elsewhere.[20] The resulting band structure along the different crystallographic directions, together with the corresponding density of states, are consistent with previous calculations.[11] It is easy then to identify the projected energy gaps in the electronic structure. In the $\overline{\Gamma M}$ direction, the main energy gap is centered around $\overline{\Gamma}$ about 2.7 eV below ε_F.[11] Although the gap disperses upwards as $k_{\parallel}$ increases, it remains below ε_F for all k values. Hence no energy gaps are present above ε_F for this azimuth, implying the wave functions associated with IPS features along this direction are expected to extend into the bulk. In the $\overline{\Gamma X}$ direction, the main energy gap is centered around $\overline{X}$, about 2 eV above ε_F. So in this direction, we expect to see some evidence of this gap, for large values of $k_{\parallel}$. From the calculation, for both azimuths, we have extracted the allowed interband transitions between unoccupied states. For a particular $k_{\parallel}$, we can find the final state energies for optical transitions, from a high lying unoccupied state when the photon energies are within the sensitivity of the detector ($\hbar\omega \simeq 9.5 \pm 0.3$ eV). In this way we can predict, based on energy conservation, the ϵ *vs* k dispersion of bulk derived resonances. Figures 3 and 6 show the prediction of these calculations as compared with experimental results.

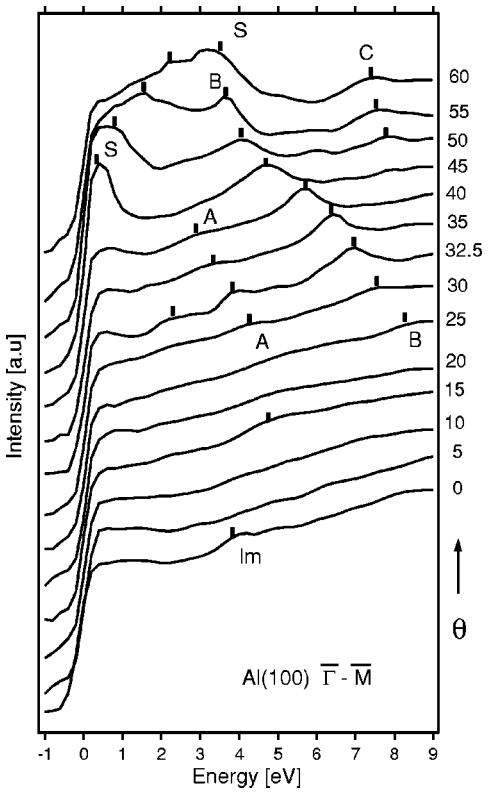

FIG. 2. IPS spectra from Al(100) along the [001] direction. The solid line is a smoothed spline fit to the data points. The image resonance and other transitions have been highlighted with vertical lines.

IV. EXPERIMENTAL RESULTS AND DISCUSSION

A. $\overline{\Gamma M}$ direction

Figure 2 shows a set of IPS spectra normalized to a common intensity at the threshold energy. Each spectrum is taken at a different angle of incidence (θ), along the $\overline{\Gamma M}$ direction. The first important feature which we have labeled as Im, has been identified in a previous report[15] as an image resonance. It is not as prominent in this surface as it has been observed in Al(111),[17,18] but nonetheless it has several features which allow us to identify it as an image resonance: its energy is slightly below the vacuum level (~200 to 500 meV) and disperses upward in energy as $k_{\parallel}$ increases.

At larger parallel momentum, we have highlighted several spectral features with a reasonable intensity above the back-

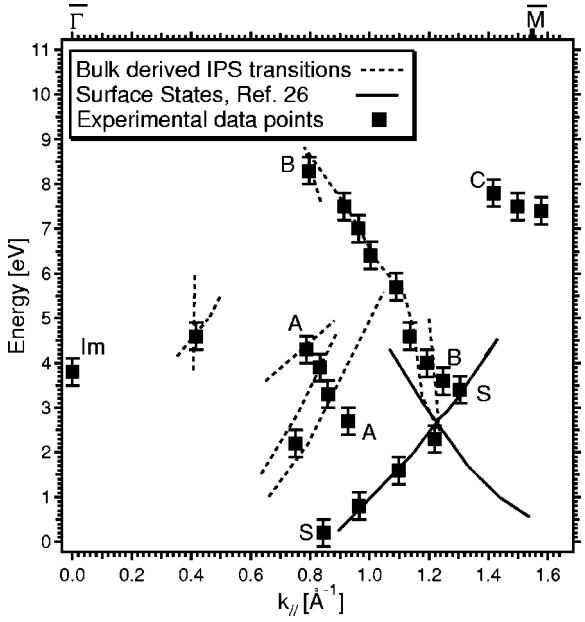

FIG. 3. Dispersion of the surface resonances as a function $k_{\|}$ along the [001] direction. The experimental data points are shown by solid squares with an error bar. The theoretical prediction for bulk derived transitions are indicated by the dashed lines. Results from calculated dispersion of surface resonances are shown with a solid line (Ref. 26).

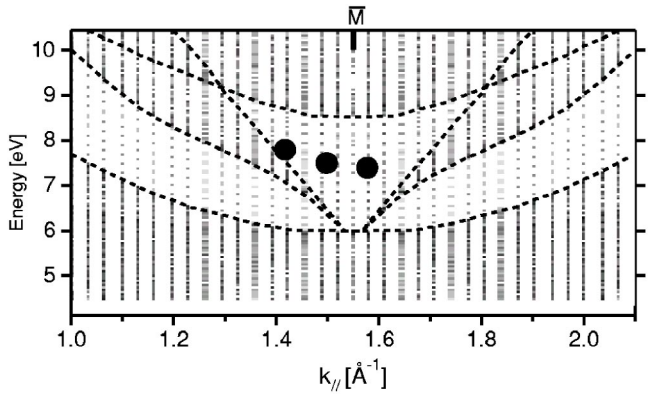

FIG. 4. Projected bulk bands onto the (100) surface along the [001] direction in k space ($\bar{\Gamma}\bar{M}$). The number of points per unit area in the $k_{\|}$ vs E plane is proportional to the number of energy states projected on to the surface. The points are generated from a calculation of the energy bands for a uniform distribution of k points inside the 3D-BZ. Lighter areas, could then be interpreted as being almost an energy band gap. The solid circles correspond to resonance *C*. The "pseudo gap" at $\bar{M}(k_{\|} \approx 1.55\ \text{Å}^{-1})$ along this azimuth, contains this surface resonance.

ground and which also show a dispersion that can be followed over consecutive spectra.

The feature centered at 3.5 eV (labeled as *A*) is well defined for $\theta \simeq 32.5°$. Away from this angle it turns into a broad and less well defined peak. Feature *B*, the most prominent peak in this azimuth, decreases in energy by about 5 eV, going from $\theta \simeq 25°$ up to 55°. At large angles there are two other features, one of them (*S*) emerges from ε_F at about 40°, disperses upwards in energy, having a strong intensity and a narrow peak shape. The second one, labeled as *C*, is detectable at about $\theta \simeq 50°$ over a very narrow angular range. It decreases slightly its energy as the angle is increased up to the detection limit of the spectrometer. Most of the features disperse down in energy as $k_{\|}$ increases. The only exception in this azimuth is *S* which moves from ε_F up to 3.5 eV for $\theta \simeq 60°$. A plot of the ε vs $k_{\|}$ dispersion of these features is shown in Fig. 3. The solid squares with error bars are the experimental points. The dashed lines, indicate the calculated final state energy and momentum of the optical transition giving rise to 9.5 ± 0.3 eV photons (i.e., within the "energy window" of our spectrometer).

By looking at the several direct transitions contributing to feature *A*, it is then clear why it broadens very fast and decreases its intensity. In the same way feature *B*, which decreases in energy from almost 8 eV to well below 4 eV, appears to follow a single bulk transition over a wide range of k values (0.7 Å^{-1}–1.1 Å^{-1}). Only for large values of $k_{\|}$ it is evident that this feature is composed of several different direct transitions. The coincidence between calculation and experimental values, in this particular case, justifies identifying *B* as a bulk derived resonance. As expected the image state is not predicted by our bulk calculation, but neither are features *S* and *C*. In Fig. 3 we have also included solid lines which are theoretical predictions from a self consistent calculation by Hummel and Bross,[26] for Al(100). It reveals two surface resonances in the energy range between ε_F and the vacuum level. There is a state which crosses ε_F at about 0.85 Å^{-1} and follows a parabolic dispersion with increasing $k_{\|}$. This resonance, shown by the solid line in Fig. 3, overlaps nicely with the experimental data points we have labeled as *S*. Resonance *S* is the continuation beyond the ε_F crossing of the occupied surface state of Al with energy of ≈ -2.7 eV at $\bar{\Gamma}$.[10,11,26] Hummel and Bross[26] predict this state continues dispersing parabolically in energy as $k_{\|}$ increases.

In general, in this azimuth there is a reasonably good agreement between predicted transitions (both surface and bulk derived resonances) and the measured IPS features. Clear exception to this statement is resonance *C*. The origin of this dispersing feature, at fairly large incidence angles, could be understood better with the help of the surface projected band structure shown in Fig. 4.

Each vertical line in Fig. 4 consists of a sequence of points representing energy states of the same $k_{\|}$ but with different $k_{\perp}$, as provided by our calculation. The higher the density of points, the higher is then the density of states projected for that particular energy. Thus, regions with lighter shades represent areas which are almost absolute band gaps. These lighter shaded areas can become "pseudo band gaps," and in a way similar as real energy band gaps, they can host surface resonances like *C*. To clarify this point we have included in the same plot, with circular markers, the experimental dispersion of surface resonance *C* around the SBZ $\bar{M}$ point. They fit within the "pseudo gap" just as a normal surface state would do in an absolute band gap. The existence of this resonance is then induced by the breaking of the 3D symmetry at the surface.

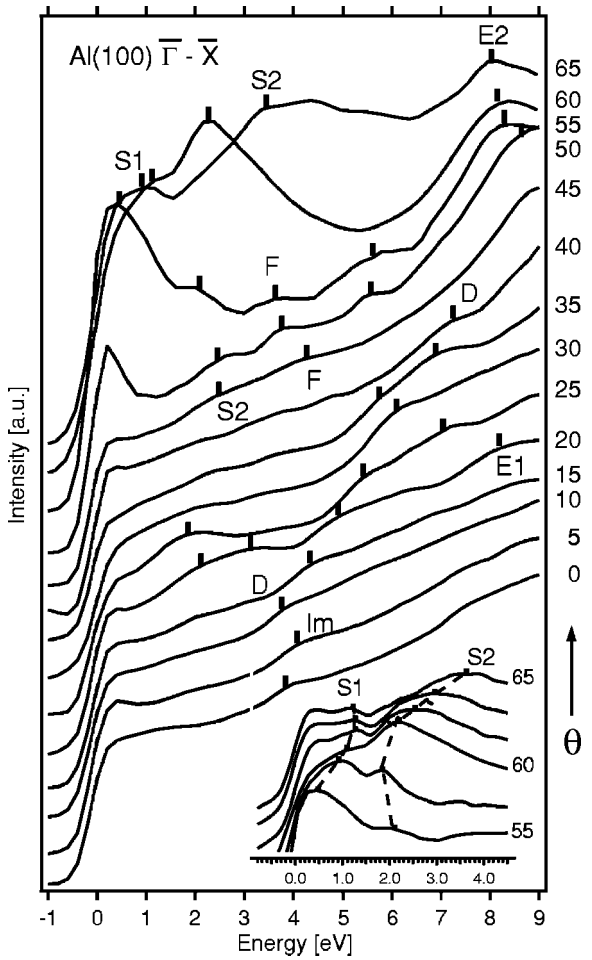

FIG. 5. IPS spectra along the [011] direction for different angles of incidence. The solid line is just a smooth spline fit to the measured data points. The insert at the bottom highlights the evolution of features *S*1 and *S*2 over a narrower angular range.

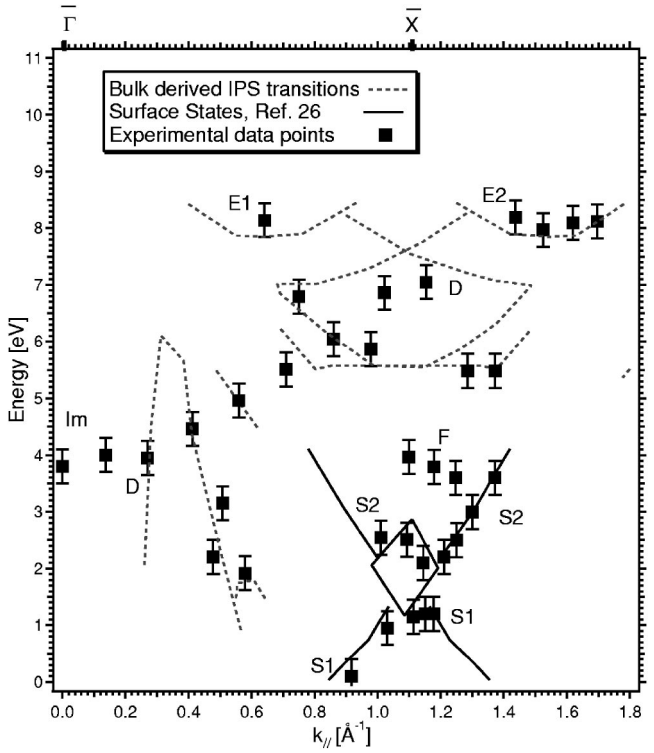

FIG. 6. Experimental resonances (black square) and bulk predicted transitions (dashed lines) along the [011] direction in *k* space. The main surface features have been highlighted. The solid lines correspond to calculated surface resonances. The split state *S* is a proper surface state only over the very small energy gap indicated by the rhombohedral contour.

B. The $\overline{\Gamma X}$ direction

In Fig. 5 we show a series of IPS spectra obtained from the Al(100) surface, but now along the $\overline{\Gamma X}$ azimuth. At normal incidence, the image resonance feature is also present in the spectrum, but as the angle increases away from $\overline{\Gamma}$ it rapidly loses intensity, becoming almost undetectable at 10° off normal. The next interesting feature (D) appears at $\theta \simeq 15°$, and $\varepsilon \approx 4.0$ eV. Although it is comparatively well defined, it changes intensity and width as it disperses up to 7.0 eV. Other salient spectral features along this direction are E and S.

As in the previous azimuth, a large resonance ($S1$) appears close to ε_F for $\theta \simeq 50°$. The evolution of this peak over a narrow angular range was rather complicated and forced us to look in more detail into their dispersion. We run a series of high resolution spectra (intensity was measured in increments of 0.1 eV), which we show as an insert at the bottom of Fig. 5. It is then easier to identify the evolution of two peaks, $S1$ and $S2$ which clearly display the opening of a gap at about 1.5 eV.

Figure 6 is an ε vs $k_{\|}$ plot of the features shown in Fig. 5. We have also added the results of our calculation for bulk allowed optical transitions, shown by the dashed lines. The solid lines indicate the dispersion of the surface resonance as predicted by the Hummel and Bross[26] calculation along this direction. The contour centered at $\overline{X}$ at an energy close to 2 eV above ε_F, corresponds to a projected energy band gap as obtained from our calculation.

It should be noted first that the apparent lack of symmetry about $\overline{X}$ exhibited by the experimental data points in Fig. 6 is inherent to the experimental technique. There is no fundamental implication on the electronic states of Al. Rather, it is simply due to a geometrical limitation of the spectrometer.

It is then easy to recognize, from Fig. 6, that features $E1$ and $E2$ are both the manifestation of a single direct transition at both sides of the SBZ $\overline{X}$ point. The upwards dispersion of resonance D and the changes in both width and intensity could be understood since D is indeed not a single transition, but corresponds to a series of different direct transition as shown by the calculated transitions in Fig. 6. Probably the most significant result is the coincidence of $S1$ and $S2$ with the calculated surface state.[26] Along this azimuth, the measured surface resonance ($S1$–$S2$) has a significant intensity in both branches, above and below the bulk band gap. Nevertheless the dominant feature is the one showing an upwards dispersion with increasing $k_{\|}$. This empty surface resonance is again the continuation of the occupied surface state with a minimum energy of ≈ 2.7 eV below ε_F at $\overline{\Gamma}$. From this mini-

mum, it follows a parabolic dispersion even beyond the closure of the gap[11] and becomes an occupied resonance. It continue its dispersion beyond ε_F, which is crossed at $k_{\|} \approx 0.8$ Å^{-1}. It becomes then an unoccupied surface state, as it intersects the bulk band gap at the zone boundary (Fig. 6). There are only very few systems in which the opening of a gap in a surface band has been identified so clearly, in particular with inverse photoemission.

In Al, there is the coincidence of both the existence of a gap at the zone boundary together with a well defined resonance, which is split at the exact location of the bulk band gap. These features are in almost perfect agreement with the surface electronic structure calculation. Indeed the split surface state is predicted to exist at the energy gap centered at 2 eV (Fig. 6) and also in its extension along the $\overline{XYM}$ direction.[26] The fact that these surface features are rather strong in Al could be related to electronic collective excitations, which should induce a maximum IPS intensity around the multipole plasmon frequency ($12.5\ \mathrm{eV}/\hbar$).[5] Surface roughness can induce a lowering of this energy for maximum emission, moving it closer to the Al surface plasmon frequency ($10.6\ \mathrm{eV}/\hbar$). This value is in fact very close to the central energy of isochromat IPS, effect which could then enhance the detection of these features close to the Fermi edge.

V. SUMMARY

We have studied using IPS the empty electronic states of Al(100) from ε_F up to 10 eV along the two main crystallographic axis ($\overline{\Gamma M}$ and $\overline{\Gamma X}$). We discovered several resonances derived from direct bulk electronic transitions, a new type of surface resonance at a "pseudo energy gap" and a surface state, linked to the occupied surface state of energy of −2.7 eV at $\overline{\Gamma}$, in a very narrow gap 2 eV above ε_F. The new surface state is split into two resonances at the bulk band gap at $\overline{X}$. LMTO calculations of the electronic structure has proven effective as a tool to recognize the origin of the different spectral features.

ACKNOWLEDGMENTS

This research was partially funded by FONDECYT Grants Nos. 1990812 and 1030198, Fundación Andes Grant No. C-10810/2 and ICM grant Chile. We thank Dr. M. Cabrera, from Departamento CMAT, UTFSM, for his help in preparing the Al crystal.

*Email address: patricio.haberle@usm.cl

[1] L. Aballe, C. Rogero, P. Kratzer, S. Gokhale, and K. Horn, Phys. Rev. Lett. **87**, 156801 (2001).
[2] L. Aballe, C. Rogero, S. Gokhale, S. Kulkarni, and K. Horn, Surf. Sci. **482-485**, 488 (2001).
[3] P. Häberle, W. Ibañez, S. R. Barman, Y. Q. Cai, and K. Horn, NIM. B **182**, 102 (2001).
[4] S. Barman, P. Häberle, K. Horn, J. Maytorena, and A. Liebsch, Phys. Rev. Lett. **86**, 5108 (2001).
[5] S. Barman, C. Stampfl, P. Häberle, W. Ibañez, Y. Cai, and K. Horn, Phys. Rev. B **64**, 195410 (2001).
[6] W. Drube, F. Himpsel, and P. Feibelman, Phys. Rev. Lett. **60**, 2070 (1988).
[7] J. Endriz and W. Spicer, Phys. Rev. Lett. **27**, 570 (1971).
[8] Y. Baer and G. Busch, Phys. Rev. Lett. **30**, 280 (1973).
[9] T. Callcott and E. Arakawa, Phys. Rev. B **11**, 2750 (1975).
[10] G. Hansson and S. Flodström, Phys. Rev. B **18**, 1562 (1978).
[11] H. Levinson, F. Greuter, and E. Plummer, Phys. Rev. B **27**, 727 (1983).
[12] S. Flodstrom, G. Hansson, S. Hastrom, and J Endriz, Surf. Sci. **53**, 156 (1975).
[13] H. Hoekstra, W. Speier, R. Zeller, and J. Fuggle, Phys. Rev. B **34**, 5177 (1989).
[14] M. Gautier, E. Marteraux, J. Durand, R. Baptist, A. Brenac, and D. Spanjaard, J. Vac. Sci. Technol. A **5**, 5177 (1986).
[15] K. Frank, H Sagner, and D. Heskett, Phys. Rev. B **40**, 2767 (1989).
[16] S. Papadia, M. Persson, and L. Salmi, Phys. Rev. B **41**, 10 237 (1990).
[17] S. Yang, R. A. Bartynski, G. P. Kochanski, S. Papadia, T. Fondén, and M. Persson, Phys. Rev. Lett. **70**, 849 (1993).
[18] S. Yang, R. A. Bartynski, and D. Vanderbilt, Phys. Rev. B **50**, 12 025 (1994).
[19] *Unoccupied Electronic States*, edited by J. C. Fuggle and J. E. Inglesfield (Springer-Verlag, Berlin, 1992).
[20] P. Häberle, W. Ibañez, R. Esparza, and P. Vargas, Phys. Rev. B **63**, 235412 (2001).
[21] G. Denninger, V. Dose, and H. Scheidt, Appl. Phys. **18**, 375 (1979).
[22] A. Goldmann, M. Donath, W. Altmann, and V. Dose, Phys. Rev. B **32**, 837 (1985).
[23] P. Erdman and E. Zipf, Rev. Sci. Instrum. **53**, 225 (1982).
[24] J. K. Grepstad, P. O. Gartland, and B. J. Slagsvold, Surf. Sci. **57**, 348 (1976).
[25] O. K. Andersen and O. Jepsen, Phys. Rev. Lett. **53**, 2571 (1984); O. K. Andersen, O. Jepsen, and D. Gloetzel, in *Highlights of Condensed Matter Theory*, edited by F. Bassani, F. Fumi, and M. P. Tosi (North–Holland, New York, 1985); O. K. Andersen, O. Jepsen, and M. Sob, in *Lecture Notes in Physics: Electronic Band Structure and Its Applications*, edited by M. Yussouff (Springer-Verlag, Berlin, 1987).
[26] W. Hummel and H. Bross, Phys. Rev. B **58**, 1620 (1998).